

## Combustion Kinetics of Biochar Prepared by Pyrolysis of Macadamia Shells

Fangyu Fan,<sup>a,b</sup> Yunwu Zheng,<sup>b</sup> Yuanbo Huang,<sup>b</sup> Yi Lu,<sup>b</sup> Zhen Wang,<sup>b</sup> Bo Chen,<sup>b</sup> and Zhifeng Zheng<sup>b,\*</sup>

The use of macadamia shells (MSs) has become an active research direction because of increasing production. This paper considers the combustion characteristics of MSs and their biochars that were investigated with thermogravimetry analysis (TGA). Combustion thermographs were obtained at different heating rates, using isoconversional methods expressed by combustion kinetics. The Kissinger-Akahira-Sunose (KAS) method authenticated the MSs, MSs-300, and MSs-600 average activation energy at 91.6 kJ/mol, 60.5 kJ/mol, and 50.1 kJ/mol, respectively. The Flynn-Wall-Ozawa (FWO) method authenticated these at 97.1 kJ/mol, 68.7 kJ/mol, and 59.5, kJ/mol. The Coats-Redfern method verified the samples combustion *via* a complex multi-step mechanism; the first stage mechanism had different activation energies at different heating rates. With increased heating rates, the activation energies of biochar decreased, and the activation energies of MSs for the second combustion zone also decreased. At the same heating rate, MSs-600 had higher activation energy values than MSs-300. The TGA curves and kinetic parameters demonstrated the superiority of the biochar derived MSs as a fuel substrate over its precursor.

*Keywords:* Macadamia Shells; Pyrolysis; Biochar; Combustion characteristics; Kinetics

*Contact information:* a: Key Laboratory for Forest Resources Conservation and Utilisation in the Southwest Mountains of China (Southwest Forestry University), Ministry of Education, Southwest Forestry University, Kunming, Yunnan, 650224, China; b: Engineering Laboratory for Highly-Efficient Utilization of Biomass, Yunnan Province; University Key Laboratory for Biomass Chemical Refinery and Synthesis, Yunnan Province; College of Materials Engineering, Southwest Forestry University, Kunming, Yunnan, 650224, China; \*Corresponding author: zhengzhifeng@swfu.edu.cn

### INTRODUCTION

The macadamia (*Macadamia integrifolia*) is a native of the rainforests of eastern Australia and is now grown in other parts of the world. At present, the worldwide production of macadamia is approximately 44,000 metric tons (kernel), and Malawi, Australia is the world's largest producer, with approximately 14,100 metric tons (Navarro and Rodrigues 2016). Currently, China has begun to develop the macadamia nut industry. Therefore, many macadamia shells (MSs) are generated during the processing of the macadamia (Bae and Su 2013). The comprehensive utilization of MSs has become an important topic.

Among different utilization methods of biomasses (Liu and Han 2015; Zhao *et al.* 2016), carbonization processes are beneficial routes that can convert biomass residues to biochar, which is attractive for energy use (Liu and Han 2015; Nizamuddin *et al.* 2015a). Two types of biochar, namely pyrolysis and hydrothermal carbonization (HTC), yield products that are obviously different in characteristics because of differences of thermo-

chemical conditions such as temperature and surroundings for HTC and pyrolysis. The yield of biochar is low and the calorific value is high *via* the pyrolysis method (Lee *et al.* 2013). In contrast, the yield of biochar is high when using the hydrothermal method, but the calorific value is low (Nizamuddin *et al.* 2015b). In this paper, the pyrolysis method was used for the preparation of biochar. In an inert atmosphere, pyrolysis technology can convert the biomass lignin, cellulose, and hemicellulose *via* complex reactions wholly into solid products with higher energy than the biomass (Chen *et al.* 2016). The biochar is a valuable product that can be used for many purposes. It is highly carbonaceous and contains a high-energy content, comparable to highly ranked coals (Thangalazhy-Gopakumar *et al.* 2015). In addition, the heterogeneous reaction of biochar with oxygen is slower than homogeneous oxidation, which is relatively safe and easy to control (Lee *et al.* 2013; Islam *et al.* 2015). For these reasons, the primary use has been as fuel for heat production for cooking and heating buildings.

As a type of biomass waste, MSs have a high oxygen content that critically limits their energy density, which is unfavorable for direct use for energy (Bae and Su 2013; García *et al.* 2015; Sadaka *et al.* 2015). Therefore, a carbonization process can improve the energy density of MSs and promote their utilization (Nizamuddin *et al.* 2016). Combustion is a way to use the biochar prepared by pyrolysis or other carbonization technologies. The combustion characteristics of the biochar from biomass are based on the main constituent of each type of biomass, such as lignin, cellulose, and hemicellulose. Knowledge of chemical composition, thermal behavior, and reactivity of the biochar is necessary for the effective design and operation of combustion application (Garcia-Maraver *et al.* 2015; Álvarez *et al.* 2016). Consequently, in the process of the combustion of biochar derived MSs, it is important to study the mechanism by which thermal degradation occurs in the different molecular fractions that store chemical energy (Conesa and Domene 2011).

Thermogravimetry analysis (TGA) is a common method to evaluate the combustion behavior and kinetics of solid samples (Islam *et al.* 2015; Xing *et al.* 2016). A representative TGA study demonstrated that the differential weight loss of samples' combustion exhibits three stages of weight loss that include dehydration, devolatilization, and biochar oxidation (Fernandez-Lopez *et al.* 2016; Nizamuddin *et al.* 2015b). The combustion weight loss shifted to higher temperature zones with increased heating rates during the nonisothermal TGA (Xing *et al.* 2016). To the best of the authors' knowledge, there have been no reports dealing with the combustion behavior and kinetics of biochar produced *via* pyrolysis of MSs.

Therefore, the objective of this preliminary work is to determine the combustion parameters of MSs and their biochars *via* thermogravimetric measurements in an oxygen atmosphere to simulate combustion conditions. At heating rates of 5 °C/min, 10 °C/min, 20 °C/min, and 40 °C/min, the adequacy of the biochar for energy are analyzed from solid state kinetic models *via* the isoconversional Kissinger-Akahir-Sunose (KAS), Flynn-Wall-Ozawa (FWO), and Coats-Redfern (CR) methods.

## EXPERIMENTAL

### Materials

The MSs were collected from the Yunnan province, China and were kept in an oven at 105 °C for 24 h to dry the samples. Dried MSs were ground to shorter than 0.6

mm fractions for the test samples. The proximate and elemental analyses are shown in Table 1.

**Table 1.** Proximate and Elemental Analyses of MSs and their Biochars

Material	Proximate Analysis (%) <sup>a</sup>			Elemental Analysis (%)				
	Volatile	Fixed Carbon	Ash	C	H	O <sup>b</sup>	N	S
MSs	77.68	19.81	2.51	52.6	6.02	40.53	0.74	0.11
MSs-300	14.68	82.43	2.89	57.69	5.82	35.52	0.88	0.09
MSs-600	9.81	87.18	3.01	60.39	5.95	32.75	0.79	0.12

Note: <sup>a</sup>- as dry basis; <sup>b</sup>- Oxygen content was obtained by difference

### Biochar preparation

Before the pyrolysis process was conducted, approximately 30 g of MSs powder was kept in the quartz boat in the cooling zone of the reactor. The flow rate of nitrogen was kept at 100 mL/min to remove the oxygen to maintain an inert atmosphere in the reactor. When the temperature reached the desired value, the quartz boat with the samples was pushed into the reacting zone for 30 min. At the end of each reaction, the quartz boat was pulled out to the cooling zone. Lastly, solid products were produced. For the purpose of investigating the combustion kinetics of the biochar prepared at different pyrolysis temperatures, temperatures were chosen at 300 °C and 600 °C. The biochar samples were designated as “MSs-XXX”, where MSs referred to macadamia shells and “XXX” represented the temperature.

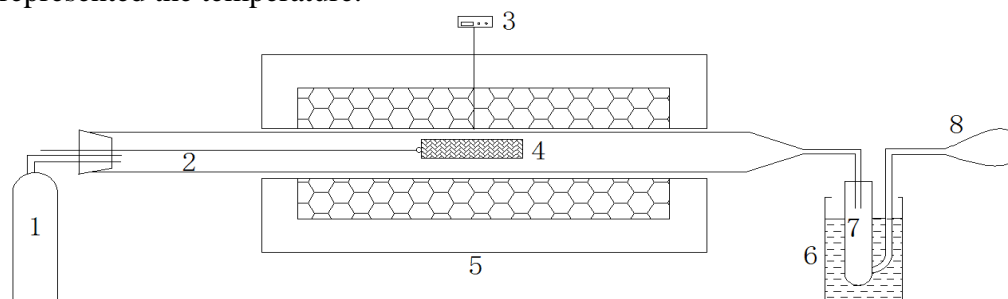


**Fig. 1.** The system of the fixed bed reactor; 1: N<sub>2</sub> gas cylinder; 2: cooling zone; 3: digital temperature controller; 4: quartz boat; 5: horizontal tubular resistance furnace; 6: liquid nitrogen condenser; 7: liquid collector; and 8: gas bag

## Methods

### Elemental and proximate analysis

The elemental analysis (C, H, N, and S) was analyzed using a Vario EL III Elemental Analyzer (Elementar, Langensfeld, Germany), and the oxygen content was calculated by the difference between CHONS. The proximate analysis was conducted using a 5E-MAG6600 Automatic Proximate Analyzer (Changsha Kaiyuan Instruments Co., Ltd, Changsha, China).

### Combustion

The combustion behavior of the samples was evaluated by thermogravimetric analysis (TGA) (NETZSCH-Gerätebau GmbH, Selb, Germany) within a temperature range of room temperature to 1000 °C, with four different heating rates (5 °C/min, 10 °C/min, 20 °C/min, and 40 °C/min). The total gas flow rate was maintained at 60 mL/min (N<sub>2</sub>: O<sub>2</sub> = 4:1).

### Calculation of the comprehensive combustibility index

The comprehensive combustibility index ( $S_N$ ) determines the combustion reactivity of the samples (Islam *et al.* 2015; Zhou *et al.* 2015), and is calculated according to Eq. 1,

$$S = \frac{(dw/dt)_{\max}(dw/dt)_{\text{mean}}}{T_i^2 T_h} \quad (1)$$

where  $(dw/dt)_{\max}$  and  $(dw/dt)_{\text{mean}}$  represent the maximum and mean rates of weight loss (wt.%/min), respectively, and  $T_i$  and  $T_h$  are the ignition and burnout temperatures (K).

### Kinetic Models

The kinetic parameters of combustion provide useful information for the design and optimization of thermo-chemical systems. Currently, there are many methods for calculating kinetic parameters (Sait *et al.* 2012; Xing *et al.* 2016). The reaction rates of the samples obey the fundamental Arrhenius equation (Eq. 2),

$$\frac{d\alpha}{dT} = \frac{A}{\beta} \exp\left(-\frac{E}{RT}\right) f(\alpha) \quad (2)$$

where  $A$  is the frequency or pre-exponential factor,  $E$  is the activation energy of the reaction (kJ/mol),  $R$  is the universal gas constant (kJ/(mol·K)),  $T$  is the absolute temperature (K),  $\beta$  is the heating rate (K/min),  $\alpha$  is the thermal conversion fraction of the samples at time  $t$ , and  $f(\alpha)$  denotes the kinetics mechanism function.

The degree of conversion,  $\alpha$ , is defined by Eq. 3,

$$\alpha = \frac{m_0 - m_T}{m_0 - m_\infty} \quad (3)$$

where  $m_0$ ,  $m_T$ , and  $m_\infty$ , are the initial, actual, and final weights of the samples, respectively.

### KAS method

The KAS (Garcia-Maraver *et al.* 2015; Islam *et al.* 2015) method is based on Eq. 4. The kinetics parameters can be obtained from a plot of  $\ln(\beta/T^2)$  versus  $1/T_\alpha$  for a given value of conversion from 0.2 to 0.8.

$$\ln\left(\frac{\beta}{T^2}\right) = \ln\left(\frac{AE}{RG(\alpha)}\right) - \frac{E}{RT_\alpha} \quad (4)$$

where  $G(\alpha)$  denotes the most probable mechanism function. Here,  $G(\alpha)$  is constant at a given value of conversion. Additionally, a first-order residence ( $n = 1$ ) is considered, which is expressed by Eq. 5,

$$G(\alpha) = n^{-1}(-1 + (1 - \alpha)^{-n}) \quad (5)$$

### FWO method

The FWO (Garcia-Maraver *et al.* 2015) method uses Doyle's approximation. The activation energy and the frequency factor are obtained at every conversion from a plot of the common logarithm of the heating rate  $\log(\beta)$  against  $1/T$ , which represents a linear

relationship with a given value of conversion at different heating rates (Eq. 6). As mentioned before in the KAS method,  $G(\alpha)$  is constant at a given value of conversion, and a first order reaction ( $n = 1$ ) was considered.

$$\log(\beta) = \log\left(\frac{AE}{RG(\alpha)}\right) - 2.315 - 0.4567 \frac{R}{T_a} \quad (6)$$

#### CR method

The CR method presents a model-free method based on an isoconversional basis to describe the thermal decomposition mechanisms for mass loss. According to the CR method (Gao *et al.* 2016), the kinetic parameters are calculated according to the logarithmic expressions of Eqs. 7 and 8,

$$\ln\left[\frac{1 - (1 - \alpha)^{1-n}}{T^2(1-n)}\right] = \ln\left[\frac{AR}{\beta E}\left(1 - \frac{2RT}{E}\right)\right] - \frac{E}{RT} \quad (n \neq 1) \quad (7)$$

$$\ln\left[-\frac{\ln(1-\alpha)}{T^2}\right] = \ln\left[\frac{AR}{\beta E}\left(1 - \frac{2RT}{E}\right)\right] - \frac{E}{RT} \quad (n = 1) \quad (8)$$

Given the temperature range and activation energies in this study,  $RT/E < 1$  and  $(1 - 2RT/E) \approx 1$ , Eqs. 9 and 10 were transformed as follows,

$$\ln\left[\frac{1 - (1 - \alpha)^{1-n}}{T^2(1-n)}\right] = \ln\left[\frac{AR}{\beta E}\right] - \frac{E}{RT} \quad (n \neq 1) \quad (9)$$

$$\ln\left[-\frac{\ln(1-\alpha)}{T^2}\right] = \ln\left[\frac{AR}{\beta E}\right] - \frac{E}{RT} \quad (n = 1) \quad (10)$$

The values of  $\ln\left[\frac{1 - (1 - \alpha)^{1-n}}{T^2(1-n)}\right]$  and  $T$  were used to calculate the TGA. The plot of  $\ln\left[\frac{1 - (1 - \alpha)^{1-n}}{T^2(1-n)}\right]$  vs.  $1/T$  ( $n \neq 1$ ), or  $\ln\left[-\frac{\ln(1-\alpha)}{T^2}\right]$  vs.  $1/T$  ( $n = 1$ ), represents a correlative straight line when the reaction order was selected appropriately. The activation energy was derived from the slope, and the pre-exponential factor  $A$  was calculated as the intercept of the straight line.

## RESULTS AND DISCUSSION

### Thermogravimetric Analysis of MSs and their Biochar

A non-isothermal TGA presents valuable thermographs that explain the combustion behavior to evaluate biomass and their char for energy (Islam *et al.* 2015). Thermographs offer information in the thermal degradation of the fuel substrates and their precursors. Thus, the combustion information is deduced for use in the design and control of the combustion system and equipment for heating application (Zhou *et al.* 2013; Garcia-Maraver *et al.* 2015).

Figures 2, 3, and 4 show the resulting TGA and DTG curves of MSs and their biochar (MSs-300 and MSs-600) combustion, with a heating rate of 5 °C/min, 10 °C/min, 20 °C/min, and 40 °C/min. These figures revealed the change in weight loss and extent of conversion patterns with increased temperature. Meanwhile, the TGA and DTG curves demonstrated the vivid influences of the heating rates on the oxidation of MSs and their biochars *via* combustion. The results demonstrated the heating rates favoured the concurrent chemical reaction mechanisms for the samples oxidation. The ignition and burnout temperatures of samples often depend on the heating rates. Both the ignition temperature and the burnout temperature became larger with the faster heating rates. Corresponding with the literatures that studied the TGA of biomass and lignite coal, their blends highlighted similar behavior as the burnout was attained (Chen *et al.* 2015; Islam *et al.* 2015)

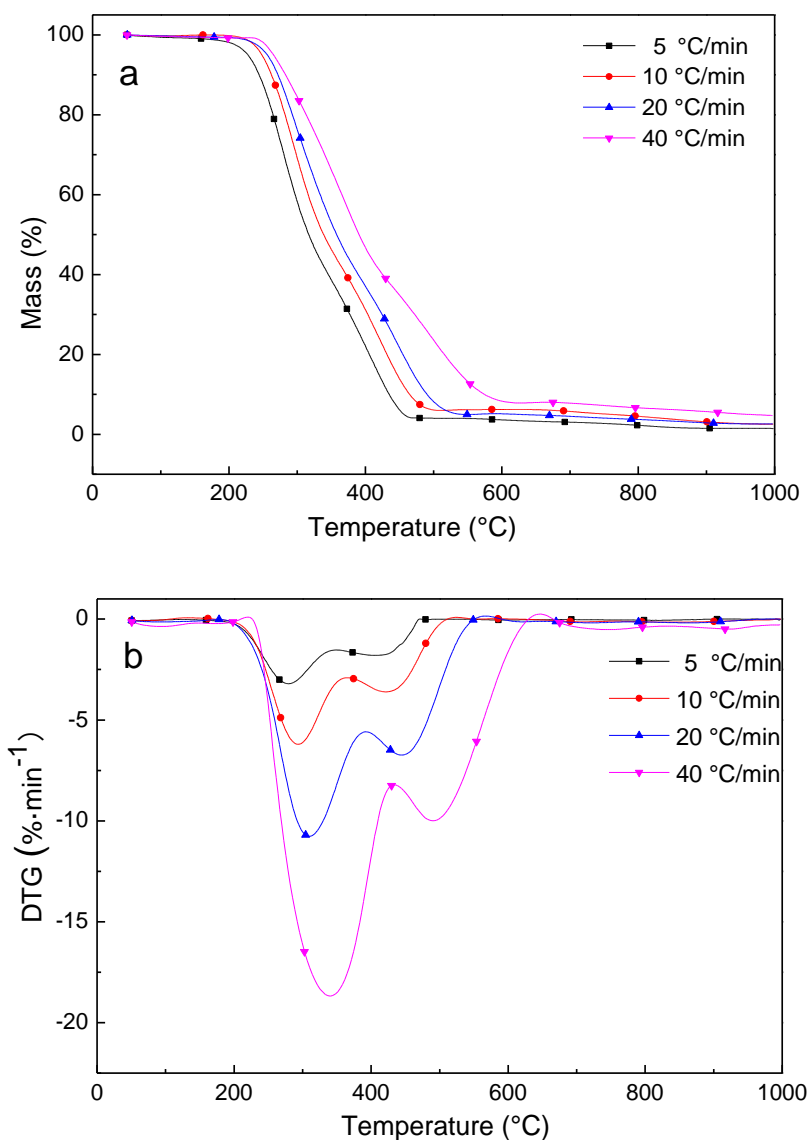


Fig. 2. a) TGA curve and b) DTG curve of MSs combustion at different heating rates

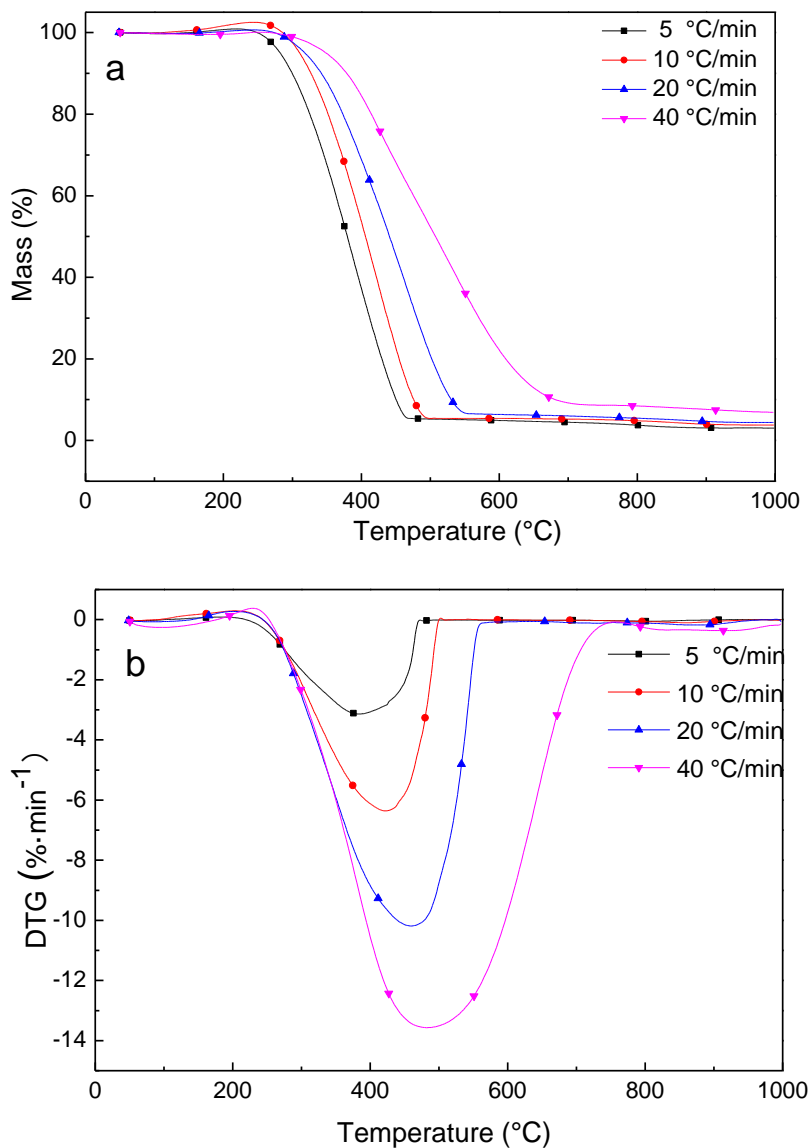
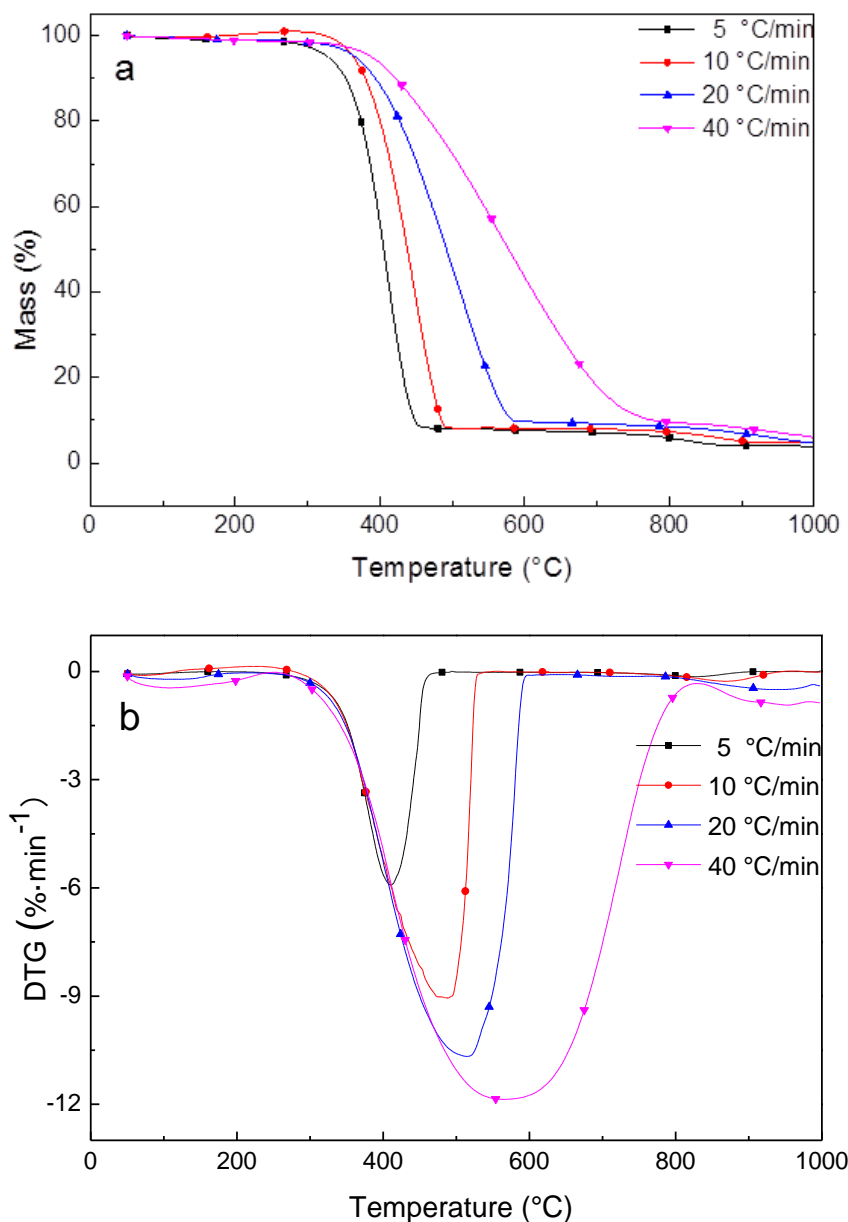


Fig. 3. a) TGA curve and b) DTG curve of MSs-300 combustion at different heating rates



**Fig. 4.** a) TGA curve and b) DTG curve of MSs-600 combustion at different heating rates

According to the TGA and DTG curves of MSs and their biochars, the curves of MSs demonstrated two distinct zones, which included the volatile matter and char combustion stage. However, the biochars curves demonstrated one zone that explained the char combustion stage. The reason was that the volatile of MSs was higher than that of the biochars, and the volatile of MSs, MSs-300, and MSs-600 were 77.68%, 14.68%, and 9.81%, respectively. The ignition temperature of the volatile is lower than fixed carbon (Buratti *et al.* 2016). As for the heating rates, the TGA and DTG curves showed a similar shape. Meanwhile, the peak in the DTG curves of all samples shifted to higher temperatures, which indicated that weight losses occurred at increased temperatures when the heating rates increased from 5 °C/min to 40 °C/min. This phenomenon is attributed to the stronger thermal shock acquired in a short time and a greater temperature gradient

between the inside and outside that the sample develops (Wang *et al.* 2012), from which the higher heat transfer limitation is derived.

### Combustion Parameters of MSs and their Biochar

The effects of the heating rates on the combustion parameters were inherent knowledge for the design and control of efficient combustion equipment. The combustion thermographs of the derivative weight loss illustrated the maximum rate of weight loss at the corresponding peak temperature. Meanwhile, the maximum and mean rates of weight loss, the ignition, and burnout temperatures could be calculated *via* TGA and DTG curves of the samples.

The combustion parameters of MSs and their biochar at four different heating rates are given in Table 2. With an increase in the heating rate, the  $S_N$  increased and the combustion performance improved, which showed that a higher heating rate was beneficial to the improvement of the combustion performance.

**Table 2.** Combustion Characteristic Parameters of MSs and their Biochars

Sample	$\beta$ ( $^{\circ}\text{C}\cdot\text{min}^{-1}$ )	$T_i$ ( $^{\circ}\text{C}$ )	$T_h$ ( $^{\circ}\text{C}$ )	$(dw/dt)_{\max}$ ( $\%\cdot\text{min}^{-1}$ )	$(dw/dt)_{\text{mean}}$ ( $\%\cdot\text{min}^{-1}$ )	$S_N \times 10^{-7}$
MSs	5	238.6	545.8	3.20	1.43	0.21
MSs	10	252.8	585.4	6.21	1.72	0.45
MSs	20	260.7	633.6	10.77	4.80	2.01
MSs	40	272.4	723.4	18.68	7.92	5.00
MSs-300	5	299.1	578.4	3.14	1.53	0.17
MSs-300	10	323.1	616.9	6.36	2.94	0.59
MSs-300	20	343.3	645.6	10.18	5.56	1.62
MSs-300	40	351.3	726.4	13.57	9.24	3.26
MSs-600	5	361.8	676.0	5.91	1.26	0.19
MSs-600	10	389.6	756.1	9.12	2.05	0.49
MSs-600	20	401.2	792.1	10.47	4.10	0.90
MSs-600	40	416.3	883.4	11.86	7.04	1.52

Compared with the MSs, the ignition and burnout temperatures of MSs-300 and MSs-600 increased at the same heating rate. The temperature increase of MSs-600 was greater than that of MSs-300. In the example of 10  $^{\circ}\text{C}/\text{min}$ , the ignition and burnout temperatures of MSs-300 were 323.1  $^{\circ}\text{C}$  and 616.9  $^{\circ}\text{C}$ . Meanwhile, the ignition and burnout temperatures of MSs-600 were 389.6  $^{\circ}\text{C}$  and 756.1  $^{\circ}\text{C}$ , respectively. This is because the higher temperatures cause decomposition of the volatile matter during the pyrolysis process (Irfan *et al.* 2016).

As shown in Table 1, MSs-300 contained higher volatile matter than MSs-600. In addition, the heating rates influenced the ignition and burnout temperatures. With an increase in the heating rates, the ignition and burnout temperatures also increased.

### Kinetics Study

The MSs and their biochars combustion kinetics were evaluated on the basis of isoconversional methods. The methods resolved the consternation of obtaining a large variance in the kinetic parameters of similar samples against other models. Figure 5 shows the results obtained *via* the isoconversional KAS and FWO methods. The activation energy values were observed to be highly dependent on the conversion, which means that the combustion of MSs and their biochar involves a complex process with

different reactions (Islam *et al.* 2015) at the same combustion stage. The results indicated that the activation energy values calculated from the KAS and FWO methods were similar for each combustion stage, and variations with the conversions were coincidental.

The MSs, MSs-300, and MSs-600 average activation energy values from the isoconversional KAS method were 91.6 kJ/mol, 60.5 kJ/mol, and 50.1 kJ/mol, respectively. The values from the isoconversional FWO method were 97.1 kJ/mol, 68.7 kJ/mol, and 59.5 kJ/mol, respectively. The average activation energy values determined by the FWO method were slightly higher than those calculated by the KAS for the same samples. The drying of the MSs before conversion to biochar, and the thermal combustion of the resultant biochar enhanced ample decomposition of the volatile component, thereby facilitating the spontaneous rate of reaction (Islam *et al.* 2015). The apparent activation energies of the three samples from the KAS and FWO were different, which can be attributed to the complex multi-step combustion mechanisms. Thus, the methods certainly clarified the dependence of the char TGA decomposition on the activation energies. The activation energies decreased with an increase in the degree of conversion. The same phenomenon is in accordance with the combustion of biochar from karanja fruit hulls by Islam *et al.* (2015). Meanwhile, the coherence or reliability of the kinetic parameters from the KAS and FWO methods were apparent from the high correlation coefficients (0.92 to 0.98).

Table 3 presents the apparent activation energies of MSs and their biochar combustion obtained by the CR method. According to the results of linear regression, using different kinetic mechanisms, the first-order combustion reaction was the most appropriate functional model, with a regression coefficient ranging from 0.922 to 0.995 (Table 3). According to all of the curve shape features of the samples, the combustion process of MSs was divided into two stages, and that of biochars as a separate stage. At the same heating rate, MSs-600 had higher values of activation energy than MSs-300. Take the example of 10 °C/min, the activation energy value of MSs-600 and MSs-300 were 88.31 kJ/mol, and 76.54 kJ/mol respectively. In addition, with an increased heating rate, the activation energies of biochar decreased, and the activation energies of MSs for the second combustion stage also decreased. With MSs-600, the activation energy decreased from 95.83 kJ/mol to 47.00 kJ/mol when the heating rate increased from 5 °C/min to 40 °C/min. This occurred because the heat transfer inside the particle was enhanced as the heating rate increased, and consequently the reactivity of the sample and its constituents were reduced in comparison to that under a lower heating rate at the same temperature (Shen *et al.* 2009).

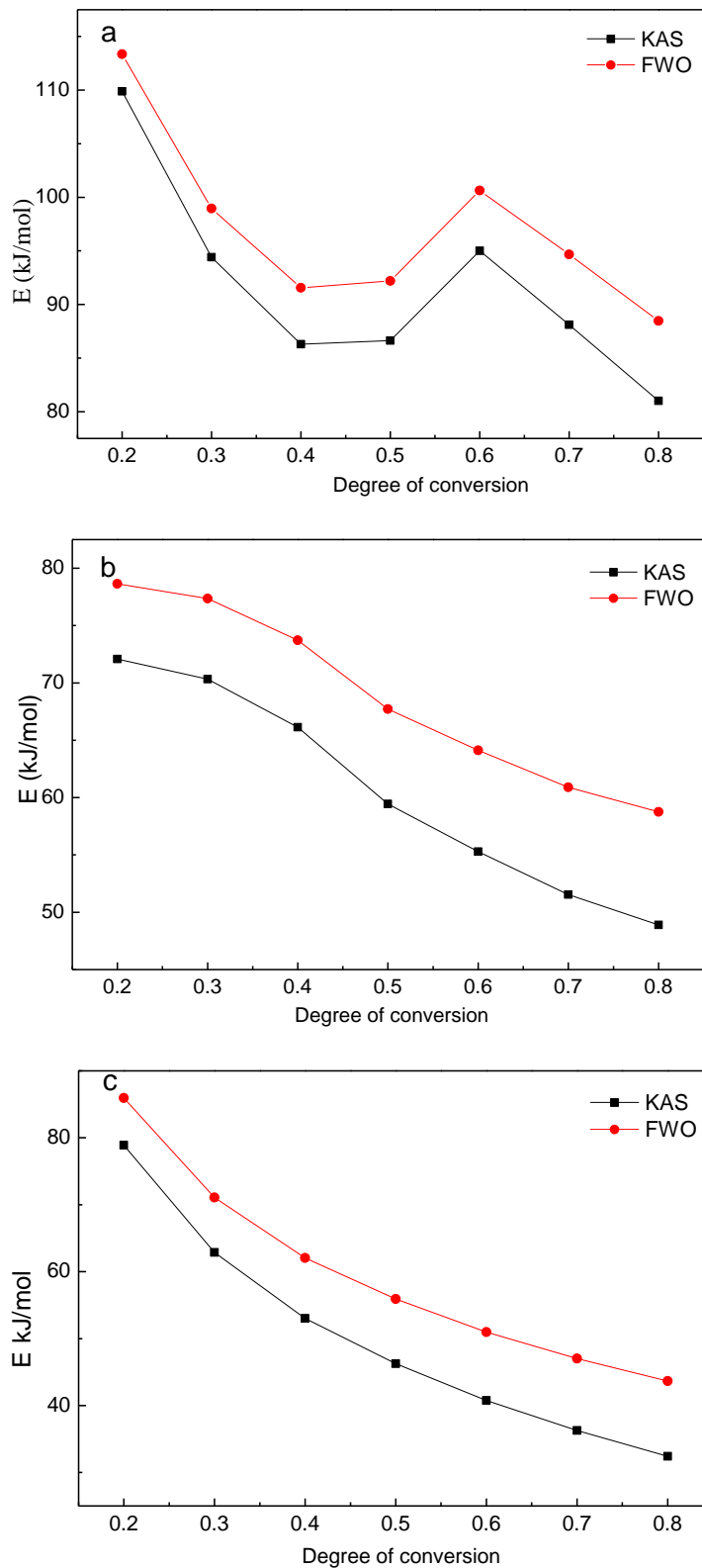


**Fig. 5.** Changes in activation energy with the progressive conversion of (a) MSs, (b) MSs-300, and (c) MSs-600 for FWO and KAS methods

**Table 3.** Kinetic Parameters of MSs and their Biochar

Materials	Heating Rates (°C·min <sup>-1</sup> )	Temperature (°C)	<i>E</i> (kJ·mol <sup>-1</sup> )	<i>A</i> (min <sup>-1</sup> )	R <sup>2</sup>
MSs	5	168 to 346	57.92	9.49 × 10 <sup>3</sup>	0.9785
		346 to 469	33.43	29	0.9733
MSs	10	185 to 367	90.80	1.64 × 10 <sup>4</sup>	0.9406
		367 to 495	32.18	34	0.9875
MSs	20	194 to 390	92.01	1.29 × 10 <sup>5</sup>	0.9647
		390 to 543	32.12	53	0.9870
MSs	40	229 to 425	62.32	4.67 × 10 <sup>3</sup>	0.9222
		425 to 626	22.96	11	0.9824
MSs-300	5	225 to 465	78.88	7.16 × 10 <sup>5</sup>	0.9769
MSs-300	10	235 to 498	76.54	2.74 × 10 <sup>5</sup>	0.9810
MSs-300	20	245- to 559	65.75	1.44 × 10 <sup>6</sup>	0.9888
MSs-300	40	262 to 726	48.67	461	0.9808
MSs-600	5	265 to 486	95.83	6.23 × 10 <sup>5</sup>	0.9770
MSs-600	10	268 to 490	88.31	1.40 × 10 <sup>6</sup>	0.9556
MSs-600	20	295 to 599	67.28	7.89 × 10 <sup>3</sup>	0.9947
MSs-600	40	298 to 791	47.00	169	0.9905

## CONCLUSIONS

1. The use of different isoconversional methods led to the calculation of activation energy of each combustion stage for MSs and their biochars, which was highly dependent on the conversion. Thus, this phenomena meant that the combustion of MSs and their biochar contained a complex process with different reactions at the same combustion stage.
2. The activation energy values calculated from the KAS and FWO methods were similar for each combustion stage, and variations in their conversion were coincidental. The activation energy values determined by the FWO method were slightly higher than those calculated by the KAS for the same samples. The KAS method authenticated the MSs, MSs-300, and MSs-600 average activation energy at 91.6 kJ/mol, 60.5 kJ/mol, and 50.1 kJ/mol, respectively. The Flynn-Wall-Ozawa (FWO) method authenticated these at 97.1 kJ/mol, 68.7 kJ/mol, and 59.5, kJ/mol
3. The CR method disclosed the firm dependence of the char combustion on a complex multi-step mechanism. At the same heating rate, MSs-600 had larger values of activation energy than MSs-300. At heating rates of 10 °C/min, the activation energy value of MSs-600 and MSs-300 were 88.31 kJ/mol, and 76.54 kJ/mol, respectively.

## ACKNOWLEDGMENTS

This work was supported by the National Natural Science Foundation of China (No. 31670599, No.31160147), the 948 project of the State Forestry Administration of China (No. 2013-4-08), the Major Project of New Energy (No. 5 [2015]), of the Yunnan Province, China, and the Major Project (No. ZD2014012) of the Education Department of the Yunnan Province, China.

## REFERENCES CITED

- Álvarez, A., Pizarro, C., García, R., Bueno, J. L., and Lavín, A. G. (2016). "Determination of kinetic parameters for biomass combustion," *Bioresource Technology* 216, 36-43. DOI: 10.1016/j.biortech.2016.05.039
- Bae, J. S., and Su, S. (2013). "Macadamia nut shell-derived carbon composites for post combustion CO<sub>2</sub> capture," *International Journal of Greenhouse Gas Control* 19(11), 174-182. DOI: 10.1016/j.ijggc.2013.08.013
- Buratti, C., Mousavi, S., Barbanera, M., Lascaro, E., Cotana, F., and Bufacchi, M. (2016). "Thermal behaviour and kinetic study of the olive oil production chain residues and their mixtures during co-combustion," *Bioresource Technology* 214, 266-275. DOI: 10.1016/j.biortech.2016.04.097
- Conesa, J. A., and Domene, A. (2011). "Biomasses pyrolysis and combustion kinetics through n -th order parallel reactions," *Thermochimica Acta* 523(1-2), 176-181. DOI: 10.1016/j.tca.2011.05.021
- Chen, J., Lin, M., Cai, J., Yin, H., Song, X., and Li, A. (2015). "Thermal characteristics and kinetics of refining and chemicals wastewater, lignite and their blends during combustion," *Energy Conversion & Management* 100, 201-211. DOI: 10.1016/j.enconman.2015.05.016
- Chen, T., Liu, R., and Scott, N. R. (2016). "Characterization of energy carriers obtained from the pyrolysis of white ash, switchgrass and corn stover - biochar, syngas and bio-oil," *Fuel Processing Technology* 142, 124-134. DOI: 10.1016/j.fuproc.2015.09.034
- Fernandez-Lopez, M., Pedrosa-Castro, G. J., Valverde, J. L., and Sanchez-Silva, L. (2016). "Kinetic analysis of manure pyrolysis and combustion processes," *Waste Management* 58, 230-240. DOI: 10.1016/j.wasman.2016.08.027
- García, R., Pizarro, C., Álvarez, A., Lavín, A. G., and Bueno, J. L. (2015). "Study of biomass combustion wastes," *Fuel* 148(12), 152-159. DOI: 10.1016/j.fuel.2015.01.079
- Garcia-Maraver, A., Perezjimenez, J. A., Serranobernardo, F., and Zamorano, M. (2015). "Determination and comparison of combustion kinetics parameters of agricultural biomass from olive trees," *Renewable Energy* 83(1), 45-50. DOI: 10.1016/j.renene.2015.05.049
- Gao, Y., Yu, B., Wu, K., Yuan, Q., Wang, X., and Chen, H. (2016). "Physicochemical, pyrolytic, and combustion characteristics of hydrochar obtained by hydrothermal carbonization of biomass," *BioResources* 11(2), 4113-4133. DOI: 10.15376/BIORES.11.2.4113-4133
- Irfan, M., Chen, Q., Yue, Y., Pang, R., Lin, Q., Zhao, X., and Chen, H. (2016). "Co-production of biochar, bio-oil and syngas from halophyte grass (*Achnatherum splendens* L.) under three different pyrolysis temperatures," *Bioresource Technology* 211, 457-463. DOI: 10.1016/j.biortech.2016.03.077
- Islam, M. A., Auta, M., Kabir, G., and Hameed, B. H. (2016). "A thermogravimetric analysis of the combustion kinetics of karanja (*Pongamia pinnata*) fruit hulls char," *Bioresource Technology* 200, 335-341. DOI: 10.1016/j.biortech.2015.09.057
- Lee, Y., Park, J., Ryu, C., Gang, K. S., Yang, W., Park, Y. K., Jung, J., and Hyun, S. (2013). "Comparison of biochar properties from biomass residues produced by slow pyrolysis at 500 °C," *Bioresource Technology* 148, 196-201. DOI: 10.1016/j.biortech.2013.08.135

- Liu, Z., and Han, G. (2015). "Production of solid fuel biochar from waste biomass by low temperature pyrolysis," *Fuel* 158, 159-165. DOI: 10.1016/j.fuel.2015.05.032
- Navarro, S. L. B., and Rodrigues, C. E. C. (2016). "Macadamia oil extraction methods and uses for the defatted meal byproduct," *Trends in Food Science & Technology* 54, 148-154. DOI: 10.1016/j.tifs.2016.04.001
- Nizamuddin, S., Jaya Kumar, N. S., Sahu, J. N., Ganesan, P., Mubarak, N. M., and Mazari, S. A. (2015a). "Synthesis and characterization of hydrochars produced by hydrothermal carbonization of oil palm shell," *Canadian Journal of Chemical Engineering* 93(11), 1916-1921. DOI: 10.1002/cjce.22293
- Nizamuddin, S., Mubarak, N. M., Tiripathi, M., Jayakumar, N. S., Sahu, J. N., and Ganesan, P. (2015b). "Chemical, dielectric and structural characterization of optimized hydrochar produced from hydrothermal carbonization of palm shell," *Fuel*, 163.88-97. DOI:/10.1016/j.fuel.2015.08.057
- Nizamuddin, S., Shrestha, S., Athar, S., Ali, B. S., and Siddiqui, M. A. (2016). "A critical analysis on palm kernel shell from oil palm industry as a feedstock for solid char production," *Reviews in Chemical Engineering* 32(5), 489-505. DOI: 10.1515/revce-2015-0062
- Sadaka, S., Liechty, H., Pelkki, M., and Blazier, M. (2015). "Pyrolysis and combustion kinetics of raw and carbonized cottonwood and switchgrass agroforests," *BioResources* 10(3), 4498-4518. DOI: 10.1537/biores.10.3.4498-4518
- Sait, H. H., Hussain, A., Salema, A. A., and Ani, F. N. (2012). "Pyrolysis and combustion kinetics of date palm biomass using thermogravimetric analysis," *Bioresource Technology* 118, 382-389. DOI: 10.1016/j.biortech.2012.04.081
- Shen, D. K., Gu, S., Luo, K. H., Bridgwater, A. V., and Fang, M. X. (2009). "Kinetic study on thermal decomposition of woods in oxidative environment," *Fuel* 88(6), 1024-1030. DOI: 10.1016/j.fuel.2008.10.034
- Thangalazhy-Gopakumar, S., Al-Nadheri, W. M. A., Jegarajan, D., Sahu, J. N., Mubarak, N. M., and Nizamuddin, S. (2015). "Utilization of palm oil sludge through pyrolysis for bio-oil and bio-char production," *Bioresource Technology*, 178, 65-69. DOI: 10.1016/j.biortech.2014.09.068
- Wang, L., Hustad, J. E., Skreiberg, O., Skjevrak, G., and Grønli, M. (2012). "A critical review on additives to reduce ash related operation problems in biomass combustion applications," *Energy Procedia* 20(5), 20-29. DOI: 10.1016/j.egypro.2012.03.004
- Xing, X., Fan, F., Shi, S., Xing, Y., Li, Y., Zhang, X., and Yang, J. (2016). "Fuel properties and combustion kinetics of hydrochar prepared by hydrothermal carbonization of corn straw," *BioResources* 11(4), 9190-9204. DOI: 10.15376/BIORES.11.4.9190-9204
- Zhao, C., Shao, Q., Ma, Z., and Zhao, X. (2016). "Physical and chemical characterizations of corn stalk resulting from hydrogen peroxide presoaking prior to ammonia fiber expansion pretreatment," *Industrial Crops & Products*, 83(2), 86-93. DOI: 10.1016/j.indcrop.2015.12.018

- Zhou, B., Zhou, J., Zhang, Q., Chen, D., Liu, X., Wang, L., Ji, R., and Ma, H. (2015). "Properties and combustion characteristics of molded solid fuel particles prepared by pyrolytic gasification or sawdust carbonized carbon," *BioResources* 10(4), 7795-7807. DOI: 10.15376/biores.10.4.7795-7807
- Zhou, Z., Hu, X., You, Z., Wang, Z., Zhou, J., and Cen, K. (2013). "Oxy-fuel combustion characteristics and kinetic parameters of lignite coal from thermo-gravimetric data," *Thermochimica Acta* 553, 54-59. DOI: 10.1016/j.tca.2012.11.030

Article submitted: January 20, 2017; Peer review completed: March 30, 2017; Revised version received: April 2, 2017; Accepted: April 3, 2017; Published: April 13, 2017.  
10.15376/biores.12.2.3918-3932